NeuroImage: Clinical 39 (2023) 103473

Contents lists available at ScienceDirect

NeuroImage: Clinical

journal homepage: www.elsevier.com/locate/ynicl

Spatial patterns of gray and white matter compromise relate to age of seizure onset in temporal lobe epilepsy

Alice Ballerini [a,b], Donatello Arienzo [b,c], Alena Stasenko [b,c], Adam Schadler [b,c], Anna Elisabetta Vaudano [a,d], Stefano Meletti [a,d], Erik Kaestner [b,c,1], Carrie R. McDonald [b,c,e,*,1]

[a] Department of Biomedical, Metabolic and Neural Science, University of Modena and Reggio Emilia, Modena, Italy
[b] Department of Psychiatry, University of California, San Diego, USA
[c] Center for Multimodal Imaging and Genetics, University of California, San Diego, USA
[d] Neurology Unit, OCB Hospital, AOU Modena, Italy
[e] Department of Radiation Medicine & Applied Sciences, University of California, San Diego, USA

ARTICLE INFO

Keywords:
Temporal Lobe Epilepsy
Superficial White Matter
Cortical Atrophy
Age of Onset

ABSTRACT

Objective: Temporal Lobe Epilepsy (TLE) is frequently a neurodevelopmental disorder, involving subcortical volume loss, cortical atrophy, and white matter (WM) disruption. However, few studies have addressed how these pathological changes in TLE relate to one another. In this study, we investigate spatial patterns of gray and white matter degeneration in TLE and evaluate the hypothesis that the relationship among these patterns varies as a function of the age at which seizures begin.

Methods: Eighty-two patients with TLE and 59 healthy controls were enrolled. T1-weighted images were used to obtain hippocampal volumes and cortical thickness estimates. Diffusion-weighted imaging was used to obtain fractional anisotropy (FA) and mean diffusivity (MD) of the superficial WM (SWM) and deep WM tracts. Analysis of covariance was used to examine patterns of WM and gray matter alterations in TLE relative to controls, controlling for age and sex. Sliding window correlations were then performed to examine the relationships between SWM degeneration, cortical thinning, and hippocampal atrophy across ages of seizure onset.

Results: Cortical thinning in TLE followed a widespread, bilateral pattern that was pronounced in posterior centroparietal regions, whereas SWM and deep WM loss occurred mostly in ipsilateral, temporolimbic regions compared to controls. Window correlations revealed a relationship between hippocampal volume loss and whole brain SWM disruption in patients who developed epilepsy during childhood. On the other hand, in patients with adult-onset TLE, co-occurring cortical and SWM alterations were observed in the medial temporal lobe ipsilateral to the seizure focus.

Significance: Our results suggest that although cortical, hippocampal and WM alterations appear spatially discordant at the group level, the relationship among these features depends on the age at which seizures begin. Whereas neurodevelopmental aspects of TLE may result in co-occurring WM and hippocampal degeneration near the epileptogenic zone, the onset of seizures in adulthood may set off a cascade of SWM microstructural loss and cortical atrophy of a neurodegenerative nature.

1. Introduction

Temporal Lobe Epilepsy (TLE) is often a debilitating disorder, affecting both gray matter (GM) and white matter (WM) networks throughout the brain (Hatton et al., 2020; Whelan et al., 2018). These pathological changes can be progressive and are intricately linked to clinical outcomes and cognitive comorbidities (Kaestner et al., 2019; Reyes et al., 2020; Stasenko et al., 2022). Thus, it is important to

Abbreviations: FA, fractional anisotropy; FX, fornix; GM, gray matter; GTC, generalized tonic-clonic seiure; HS, hippocampal sclerosis; ICV, intracranial volume; L-TLE, left temporal lobe epilepsy; MD, mean diffusivity; MTL, medial temporal lobe; PHC, parahippocampal cingulum; R-TLE, right temporal lobe epilepsy; SWM, superficial white matter; TBV, total brain volume; TLE, temporal lobe epilepsy; UNC, uncinate fasciculus; WM, white matter.

* Corresponding author at: UC San Diego Altman Clinical and Translational Research Institute, 9452 Medical Ctr Dr, La Jolla 92037, CA, USA.
E-mail address: camcdonald@health.ucsd.edu (C.R. McDonald).

[1] Both authors contributed equally as senior authors.

https://doi.org/10.1016/j.nicl.2023.103473
Received 29 April 2023; Received in revised form 29 June 2023; Accepted 6 July 2023
Available online 8 July 2023

understand the origins and the disease mechanisms that contribute to GM and WM pathology in TLE.

TLE can begin at any point in life and lead to abnormalities in brain structure and function. However, the brain is particularly vulnerable to the effects of epilepsy during childhood (Beghi, 2020). As a result, age of seizure onset has important implications for understanding patterns of GM and WM pathology and how they relate to one another. In particular, recurrent seizures early in life, during a period of heightened plasticity and brain development, may disrupt WM myelination and/or interfere with synaptic pruning in neocortex leading to structural abnormalities in the WM and GM, respectively (Bencurova et al., 2022; Blümcke et al., 2013; Hermann et al., 2002). These changes may occur globally, or they may be more pronounced proximal to the seizure focus. Conversely, when seizures begin in adulthood, they may lead to different patterns of GM and WM vulnerability because of decreases in brain plasticity in the fully developed brain (Doucet et al., 2015).

Despite accumulating evidence for the presence of broad cortical thinning (Larivière et al., 2020; McDonald et al., 2008), subcortical volume loss (Whelan et al., 2018), and WM compromise in TLE (Hatton et al., 2020; Stasenko et al., 2022), studies investigating how GM and WM pathologies are related to one another are limited (Chang et al., 2019; Liu et al., 2016; Winston et al., 2020). Neocortical GM appears to follow a widespread multi-lobar and bilateral pattern of atrophy in TLE (Galovic et al., 2019; Larivière et al., 2020; McDonald et al., 2008). Conversely, there is some evidence that limbic WM damage is more pronounced in the ipsilateral hemisphere and is greatest close to the seizure focus (Hatton et al., 2020; Urquia-Osorio et al., 2022). However, because GM and WM developmental trajectories differ markedly early in life (Bethlehem et al., 2022), associations between the two may differ as a function of when seizures begin. Indeed, WM pathology has been shown to be more pronounced in those with an early seizure onset (Nagy et al., 2016), and there is evidence that injury to the WM sub-adjacent to the neocortex (i.e., the superficial white matter; SWM) is related to hippocampal sclerosis (HS) (Liu et al., 2016) — another feature associated with early seizure onset in TLE. However, the presence of HS has also been associated with broad patterns of cortical thinning, suggesting a relationship between hippocampal and cortical damage in TLE (Bonilha et al., 2010; Mueller et al., 2009). To date, studies that have investigated the spatial patterns of atrophy in cortical thickness and SWM (Chang et al., 2019; Liu et al., 2016; Winston et al., 2020) hint that different biological processes are likely driving these two types of injury in TLE. However, these studies did not directly explore the role of the age of seizure onset and test how the age at which seizures begin influences cortical-subcortical GM atrophy relationships with WM disruption.

Our study aims to extend knowledge about the processes underlying GM and WM atrophy across the developmental spectrum using structural and diffusion MRI. First, we examine patterns of subcortical and cortical GM atrophy and WM microstructural loss in a large group of individuals with drug-resistant TLE compared to healthy controls. Next, we characterize how these pathologies spatially correlate in TLE. Finally, we explore whether GM and WM atrophy relationships vary across different ages of seizure onset. We test this by measuring changes not only in neocortical thinning and subcortical GM, but also in both the SWM and deep WM tracts, leading to a comprehensive analysis of neuroanatomical relationships in TLE.

2. Materials and methods

2.1. Participants

Eighty-two patients with focal TLE [mean age 35.85(±12.95), 44 females] and 59 healthy controls [mean age 36.95(±13.72), 36 females] were enrolled from the UC San Diego and UC San Francisco Epilepsy Centers. The TLE diagnoses were established by board-certified neurologists with expertise in epileptology, according to the criteria defined by International League Against Epilepsy (ILAE, (Fisher et al., 2017; Scheffer et al., 2017)). Forty-three out of 82 patients were classified as left TLE (L-TLE), and 39 were classified as right TLE (R-TLE) based on video-EEG telemetry, clinical history, seizure semiology, and neuroimaging evaluation. The MRI images were visually inspected by a board-certified neuroradiologist with expertise in epileptology, in order to detect the presence of HS. Patients with and without HS were enrolled in this study; however, we excluded patients with space-occupying lesions (e.g., focal cortical dysplasia, tumors).

2.2. Image acquisition

MRI sequences were performed on a General Electric Discovery MR750 3 T scanner with an 8-channel phased-array head coil at either UCSD or UCSF. Both centers used a prospectively harmonized and identical MRI acquisition that included a conventional three-plane localizer, GE calibration scan, a T1-weighted 3D structural scan (TR = 8.08 ms, TE = 3.16 ms, TI = 600 ms, flip angle = 8°, FOV = 256 mm, matrix = 256 × 192, slice thickness = 1 mm), and for diffusion, a single-shot pulsed-field gradient spin-echo EPI sequence (TE/TR = 80.4 ms/8 s; FOV = 240 mm, matrix = 128 × 128 × 53; axial). Diffusion-weighted images were acquired with b = 0 and b = 1000 mm^2/s with 30 diffusion gradient directions. Two additional b = 0 volumes were acquired with either forward or reverse phase-encode polarity for use in B0 correction. Both T1w and DWI data were preprocessed using a multimodal imaging processing pipeline developed for the *Adolescent Brain Cognitive Development* study, according to Hagler et al., 2019.

2.3. Image processing

T1-weighted image processing: Automatic segmentation of T1-weighted images was performed with FreeSurfer (v7.1.1, Fischl, 2012). From the structural MRI, 16 subcortical volumes were segmented and 68 cortical regions of interest (ROIs) were parcellated and cortical thickness was derived based on the Desikan-Killiany atlas (Desikan et al., 2006). Visual inspections of morphometric segmentations were conducted following standardized FreeSurfer protocols.

Diffusion-weighted imaging processing: The diffusion MRI images were corrected for spatial and intensity distortions due to B0 magnetic field inhomogeneities, eddy current distortion, gradient nonlinearity distortion, and head motion using FSL's TOPUP (Andersson et al., 2003; Smith et al., 2004). The reverse gradient method was used to correct B0 distortion (Holland et al., 2010). A method using least squares inverse and iterative conjugate gradient descent was used to correct for eddy currents (Zhuang et al., 2006). Distortions due to gradient nonlinearity were corrected for each frame of the diffusion data (Jovicich et al., 2006). Head motion was corrected by registering each frame to the parameters obtained through diffusion tensor fitting, accounting for variation in image contrast across diffusion orientations (Hagler et al., 2009). DMRI-derived fractional anisotropy (FA) and mean diffusivity (MD) were calculated based on a tensor fit to the b = 1.000 data.

Fiber tract FA and MD values were analyzed for three bilateral fiber tracts of interest [i.e., uncinate fasciculus (UNC), parahippocampal cingulum (PHC) and fornix (FX)]. These three tracts were selected due to their connectivity with the hippocampus/medial temporal lobe (MTL) and evidence that they are particularly affected in TLE (Hatton et al., 2020; Stasenko et al., 2022). FA and MD for each track was extracted using AtlasTrack, a probabilistic diffusion tensor atlas validated in healthy controls and TLE patients (Hagler et al., 2009). For each participant, the T1-weighted structural images were nonlinearly registered to a common space and the respective diffusion tensor orientation estimates were compared to the atlas. This resulted in a map of the relative probability that a voxel belongs to a particular tract given its location and similarity of diffusion orientation. Voxels identified with Freesurfer (v7.1.1) as cerebrospinal fluid or GM were excluded from the

fiber ROIs. Average of the diffusion parameters was calculated for each fiber ROI, weighted by fiber probability, so that voxels with low probability of belonging to a given fiber contributed minimally to average values.

SWM FA and MD were collected for the same 68 Desikan-Killiany ROIs as was obtained for the cortical thickness. FA and MD for SWM were calculated at each vertex using seven samples in 0.2 mm increments along the vector normal to the GM/WM boundary surface, from 0.8 mm to 2 mm inwards into *peri*-cortical white matter. Multiple samples were collected to account for passing through multiple voxels with varying properties. In order to minimize the effects of partial voluming and regional variations, we calculated weighted averages of FA and MD based on the proportion of GM or WM in each voxel using Tukey's bi-square weight function (Beaton & Tukey, 1974) to down weight the contribution of voxels with a low proportion of the tissue of interest. Average FA and MD measured in the WM directly beneath GM ROIs in each individual's native space (Elman et al., 2017). The method is described in detail in Elman et al., 2017. All analyses described below were performed at the ROI level and based on unsmoothed data.

2.4. Statistical analysis

Demographic and clinical variables: One-way ANOVAs and Chi-square tests were conducted to explore differences between TLE and controls, and between L-TLE and R-TLE, in demographic and clinical variables' distribution. Statistical significance for all tests was set at $p < .05$.

Ipsilateral vs *contralateral hemisphere*: After inspection of the spatial maps to ensure similar SWM, cortical, and subcortical patterns in patients with L-TLE and R-TLE (see **Supplementary Figure 1**), the cortical and subcortical ROIs for the R-TLEs were flipped, thus ipsilateral structural and diffusion data were projected on the left hemisphere and contralateral data are projected on the right hemisphere for all patients. This procedure allowed us to maximize power and consider ipsi- and contralateral differences as our primary variables. Thus, all the following analyses are reported as ipsi- or contralateral with respect to the seizure focus. Of note, the flipping was performed after each feature was z-scored relative to control values for each respective hemisphere, accordingly to the literature (Horsley et al., 2022; Larivière et al., 2022; Winston et al., 2020) and ensuring that there were no hemispheric asymmetries for cortical thickness, subcortical volumes, SWM (FA/MD), and WM tracts (FA/MD) in the control population (Supplementary Table 2).

Topography of GM and WM structures: All brain measures were converted into z-scores based on the mean and the standard deviation of the control cohort. In order to control for differences in brain size, subcortical volumes were divided by total intracranial volume (ICV) for each subject. An inspection of brain asymmetry in controls was performed by a paired sample *t*-test. All analyses that follow were performed using SPSS software 28 (IBM, Chicago, IL) or R-package software, and statistical significance for all tests was set at $p < 0.05$. Significant p-values were considered those that survived a 5% FDR correction (Benjamini & Hochberg, 1995). Whole brain differences between TLE and controls were examined in GM (i.e., cortical thickness and subcortical volumes) and WM (i.e., SWM and deep WM tracts) using multivariate analyses of covariance (MANCOVAs) models with age and sex included as covariates in all comparisons (Whelan et al., 2018).

Relationship between GM and SWM: To assess the relationships among cortical thinning, hippocampal volume, and SWM damage, partial Pearson correlations were performed for each ROI with age and sex as covariates.

Effects of age of seizure onset: To test the association between age of seizure onset and regional GM-SWM atrophy associations, we performed a series of sliding window correlations (Schulz & Huston, 2002). This procedure involves computing correlations in overlapping successive windows across a clinical variable distribution (e.g., across age of the seizure onset), revealing fluctuations in the degree, and direction of the correlation. We ranked participants according to their clinical variable (e.g., from lowest age of seizure onset to highest). The correlation was computed for successive samples of 25 participants at a time, starting from the first 25, and then proceeding up the variable level rank order, always including the next patient and excluding the first patient of the previous interval (**Supplementary Figure 2**). A window size of 25 was chosen to enhance stability of the correlation values. We excluded 6 patients from the analysis who had an age of epilepsy onset > 40 years old (age of onset 42–68 years), because there were not enough patients in this cohort for the sliding window to yield stable results. Additionally, we applied this approach to a random rank order of values to ensure that the correlation values obtained in the prior analyses were not due to chance. This approach has much in common with bootstrapping and clustering approaches (Allen et al., 2014; Shakil et al., 2018). Finally, we considered a window significant if three consecutive windows produced a significant effect. With this approach, we also explored the relationship between the ipsilateral SWM FA/MD and ipsilateral hippocampal volume. All plots were smoothed with the 'zoo' package in R, using a moving average value of five and a step of one.

To avoid overfitting due to the high number of ROIs in the Desikan-Killiany atlas, for this analysis we clustered the 68 cortical ROIs into three major groups: (I) MTL, including the entorhinal cortex, parahippocampal cortex, and the fusiform gyrus; (II) lateral temporal lobe (LTL), including the inferior, the middle, and the superior temporal gyri, banks of superior temporal sulcus, and transverse temporal gyrus; (III) extra-temporal regions, which included all the ROIs within the frontal, parietal, and occipital lobes.

3. Results

3.1. Demographic and clinical variables

Controls and patients with TLE did not significantly differ in age, sex, total brain volume (TBV), and ICV. Patients had significantly lower education compared to controls ($p < 0.001$). Forty-seven out of 82 patients had HS, whereas the rest had a normal MRI. Most of the patients were on polytherapy (82%). The number of reported lifetime generalized tonic-clonic (GTC) seizures is reported in Table 1. Age, age of

Table 1
Clinical and demographic variables in TLE and controls.

	TLE (N = 82)	Controls (N = 59)	Stat.	Sig.
Age	35.85(±12.95)	36.95(±13.72)	0.483 ^{t}	0.630
Sex (f/m)	44/38	36/23	0.757^{X}	0.384
Education (y)	13.30(±2)	16.03(±2.27)	7.549 ^{t}	<0.001***
ICV (mm^3)	990814.46 (±114529.56)	1024829.31 (±97008.95)	1.852 ^{t}	0.066
TBV (mm^3)	1128922.23 (±128259.49)	1169104.87 (±107476.90)	1.961 ^{t}	0.052
HS (yes/no)	47/35	–		
Age of epilepsy onset (y)	20.72(±14.30)	–		
Epilepsy duration (y)	15.13(±14.21)	–		
ASMs (mono/poly)	15/67	–		
GTC lifetime frequency (%)				
0–1	25.6%	–		
2 to 9	34.1%	–		
10 to 39	22%	–		
>40	14.6%	–		
N/A	3.7%	–		

Data are presented in means (±standard deviations). y: years, ICV: intracranial volume, TBV: total brain volume, HS: hippocampal sclerosis, ASM: anti-seizure medication, GTC: generalized tonic-clonic seizure, N/A: not available. ^{t}: independent sample *t*-test, ^{X}: Chi-squared test, ***: $p < .001$.

epilepsy onset, and years of epilepsy duration were strongly related to one another (**Supplementary Figure 3**). A density plot for the age of seizure onset and years of epilepsy duration is provided in **Supplementary Figure 4**.

We did not find any significant differences between L-TLE and R-TLE patients in the clinical and demographic variables. All results are summarized in Table 1 and in Supplementary Table 1.

Given that the patterns of ipsilateral and contralateral cortical, subcortical and diffusion alterations reported below were similar for L-TLE and R-TLE (**Supplementary Figure 1**) and to maximize power, we combined these two groups for all analyses.

3.2. Topography of gray and white matter structures

Whole brain cortical thickness comparison between TLE patients and controls is shown in Fig. 1**A**. Significantly thinner cortex for patients was found in posterior brain regions, particularly the bilateral precuneus [Ipsi: ($F_{(1,140)}$ = 18.928, p_{FDR} = 0.001, η^2 = 0.121), Contra: ($F_{(1,140)}$ = 17.267, p_{FDR} = 0.001, η^2 = 0.112)], the pre-central [Ipsi: ($F_{(1,140)}$ = 8.908, p_{FDR} = 0.013, η^2 = 0.061), Contra: ($F_{(1,140)}$ = 9.486, p_{FDR} = 0.011, η^2 = 0.065)] and the post-central [Ipsi: ($F_{(1,140)}$ = 11.338, p_{FDR} = 0.007, η^2 = 0.076), Contra: ($F_{(1,140)}$ = 11.108, p_{FDR} = 0.007, η^2 = 0.074)] gyri. Cortical thinning in the superior temporal gyrus was observed bilaterally [Ipsi: ($F_{(1,140)}$ = 9.905, p_{FDR} = 0.010, η^2 = 0.068), Contra: ($F_{(1,140)}$ = 5.800, p_{FDR} = 0.045, η^2 = 0.041)], while the middle temporal gyri was thinner only ipsilaterally ($F_{(1,140)}$ = 6.696, p_{FDR} = 0.032, η^2 = 0.047) (Fig. 1**A**). The MTL did not show any significant differences in TLE compared to controls. As expected, the ipsilateral hippocampal volume was lower in TLEs compared to controls ($F_{(1,140)}$ = 19.878, p_{FDR} < 0.001, η^2 = 0.127) (Fig. 1**A**).

Fig. 1**B** displays the whole brain SWM comparison between TLE patients and controls, and the significant results are summarized in Table 2 and in Supplementary Table 3. The SWM showed a spatially different pattern of alterations compared to the cortical thickness; decreased FA and increased MD was observed in TLE patients in the ipsilateral hemisphere only, with significant reductions in FA in the ipsilateral medial and inferior temporal lobe. This pattern of ipsilateral SWM loss was more extensive for MD, with increased MD that extended beyond the temporal lobe into the orbitofrontal, cingulate, and insular SWM (Supplementary Table 3).

Finally, Fig. 1**C** and Table 2 displays FA and MD standardized values for the three bilateral tracts and comparisons between patients and controls. The PHC and UNC showed a lower FA in both hemispheres, but more pronounced decreases in FA in each ipsilateral tract. All three fiber tracts showed increased MD in the ipsilateral tract compared to controls.

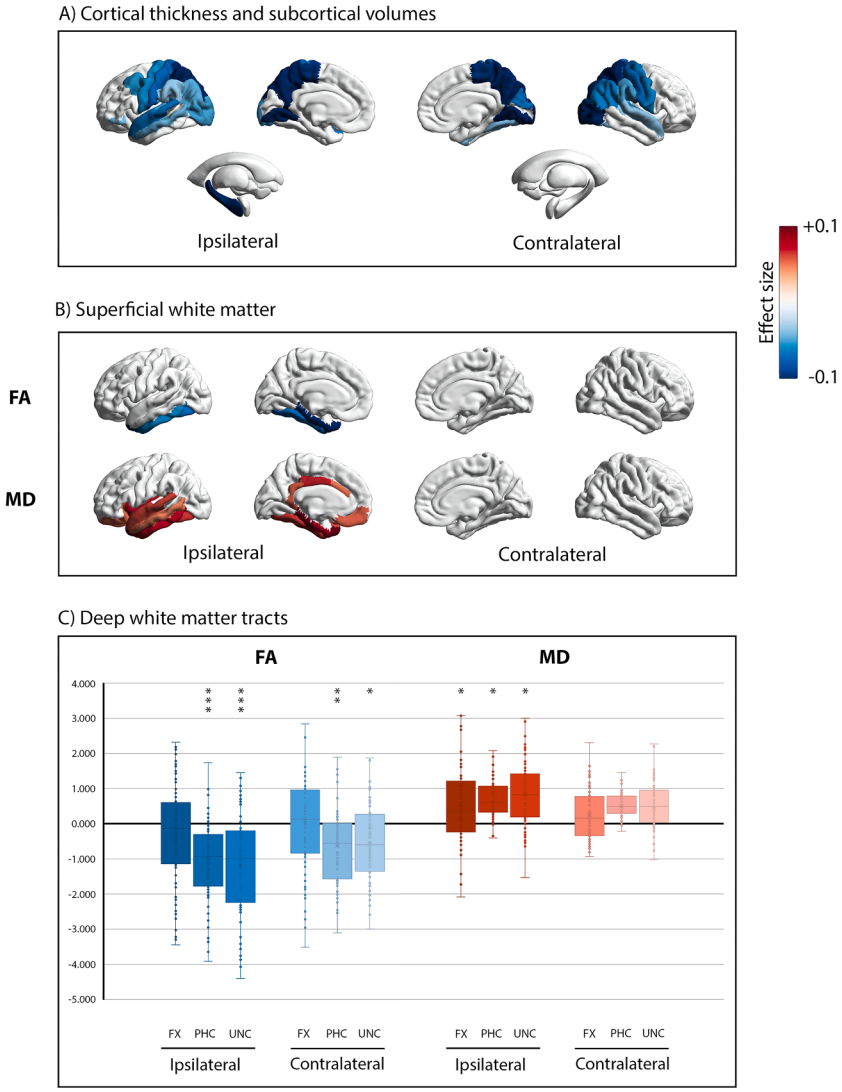

Fig. 1. *Whole brain comparison between TLE and controls.* Panel A) visualizes significant group differences in cortical thickness and subcortical volume. Panel B) shows significant group differences of superficial white matter fractional anisotropy (FA) above, and mean diffusivity (MD) below. Data for each comparison are presented as effect size (Partial Eta Squared, η^2). Blue colors (-0.1) represent the regions where TLE showed atrophy, or lower FA values, compared to controls; red colors (+0.1) represent the regions where TLE showed hypertrophy, or higher MD values, compared to controls. Only effect sizes associated with p-values that survived FDR correction (i.e., p_{FDR} < 0.05) are presented in panels a) and b). Finally, panel C) shows box-and-whisker plots of deep white matter tracts, standardized relative to controls. The central horizontal line of the boxes marks the median of the sample, the upper and lower edges of the box (the hinges) mark the 25th and 75th percentiles (the central 50% of the values fall within the box). The open circles represent individual patients. The "x" in the middle of each box marks the mean values for each fasciculus. The black line on value 0 designates the mean volume of controls. The "*" on the box indicates the significant results of the MANCOVA analysis (*: p_{FDR} < 0.05, **: p_{FDR} < 0.01, ***: p_{FDR} < 0.001). FX: fornix fasciculus, PHC: parahippocampal cingulum bundle, UNC: uncinate fasciculus. Brain maps in panel A) and B) were created by using the ENIGMA-Toolbox (Larivière et al., 2021). (For interpretation of the references to colour in this figure legend, the reader is referred to the web version of this article.)

Table 2
Group comparisons between TLE and controls in superficial and deep white matter.

	TLE	Controls	F	Sig.$_{FDR}$	η^2
Superficial white matter					
Ipsilateral superior temporal$_{MD}$	0.806 (±0.069)	0.772 (±0.032)	9.797	0.016*	0.068
Ipsilateral middle temporal$_{MD}$	0.810 (±0.062)	0.782 (±0.029)	7.538	0.033*	0.053
Ipsilateral inferior temporal$_{FA}$	0.237 (±0.045)	0.254 (±0.032)	8.987	0.037*	0.062
Ipsilateral inferior temporal$_{MD}$	0.825 (±0.057)	0.791 (±0.026)	11.645	0.010*	0.079
Ipsilateral entorhinal cortex$_{FA}$	0.219 (±0.052)	0.259 (±0.060)	17.472	0.001**	0.115
Ipsilateral entorhinal cortex$_{MD}$	0.907 (±0.114)	0.832 (±0.113)	12.271	0.015*	0.083
Ipsilateral fusiform$_{FA}$	0.233 (±0.048)	0.256 (±0.036)	10.736	0.018*	0.074
Ipsilateral fusiform$_{MD}$	0.795 (±0.053)	0.771 (±0.029)	10.465	0.013*	0.072
Ipsilateral parahippocampal cortex$_{FA}$	0.257 (±0.061)	0.299 (±0.047)	20.278	<0.001***	0.131
Ipsilateral parahippocampal cortex$_{MD}$	0.864 (±0.095)	0.796 (±0.081)	21.996	<0.001***	0.140
Ipsilateral temporal pole$_{FA}$	0.212 (±0.041)	0.240 (±0.035)	22.075	<0.001***	0.141
Ipsilateral temporal pole$_{MD}$	0.906 (±0.075)	0.856 (±0.041)	23.710	<0.001***	0.149
Deep white matter					
Ipsilateral FX$_{FA}$	0.335 (±0.040)	0.344 (±0.028)	3.221	0.087	0.023
Ipsilateral FX$_{MD}$	1.156 (±0.213)	1.067 (±0.156)	8.612	0.034*	0.060
Contralateral FX$_{FA}$	0.346 (±0.041)	0.346 (±0.028)	0.002	0.967	0.000
Contralateral FX$_{MD}$	1.105 (±0.193)	1.064 (±0.170)	2.160	0.158	0.016
Ipsilateral PHC$_{FA}$	0.337 (±0.049)	0.375 (±0.032)	24.405	<0.001***	0.153
Ipsilateral PHC$_{MD}$	0.850 (±135)	0.777 (±0.089)	11.746	0.014*	0.080
Contralateral PHC$_{FA}$	0.353 (±0.050)	0.379 (±0.049)	9.479	0.010*	0.066
Contralateral PHC$_{MD}$	0.826 (±0.124)	0.769 (±0.140)	6.747	0.052	0.048
Ipsilateral UNC$_{FA}$	0.393 (±0.037)	0.424 (±0.023)	28.200	<0.001***	0.173
Ipsilateral UNC$_{MD}$	0.828 (±0.074)	0.788 (±0.42)	11.934	0.026*	0.081
Contralateral UNC$_{FA}$	0.407 (±0.032)	0.414 (±0.051)	7.498	0.018*	0.053
Contralateral UNC$_{MD}$	0.807 (±0.070)	0.787 (±0.058)	4.004	0.083	0.027

Data are presented in means (±standard deviations). FA: fractional anisotropy, MD: mean diffusivity, FX: fornix, PHC: parahippocampal cingulum, UNC: uncinate. *: $p_{FDR} < 0.05$, **: $p_{FDR} < 0.01$, ***: $p_{FDR} < 0.001$.

3.3. Relationship between GM and SWM

Because the deep WM tract FA/MD values mirrored those of the SWM but are not in spatial alignment with the cortical ROIs, we limited our correlational analysis to GM-SWM associations. We did not find any significant linear correlations between cortical thickness and SWM FA/MD for any ROI in patients. However, sliding window correlations across the age of epilepsy onset and the years of the illness duration revealed a more complex pattern. Lower hippocampal volumes were associated with higher SWM MD across all ROIs in those TLE with an early age of seizure onset (Fig. 2**A**). There was no association between hippocampal volumes and cortical thinning. Conversely, decreases in cortical thickness were associated with increases in SWM MD in the ipsilateral MTL only (Fig. 2**B**), but only in patients with a later age of seizure onset (i.e., >20 years old) and a shorter epilepsy duration (see **Supplementary Figure 5** for sliding window correlations with disease duration). This relationship was not found in the other regions. In the contralateral hemisphere, extra-temporal cortical thinning was associated with higher SWM MD in a restricted time window for those with a very early onset (Fig. 2**C**).

The bootstrapping random rank order of values approach adopted confirmed that the correlation values obtained were not due to chance. All correlation coefficients and p-values for each sliding windows comparison are reported in Supplementary Table 4 and means and standard deviations of the age of onset and the years of epilepsy duration for each window correlation are plotted in **Supplementary Figure 6**.

3.3.1. Effects of early and late age of epilepsy onset

Because associations between GM and SWM alterations in TLE appear to depend on the age of seizure onset, we investigated whether patients with an onset during childhood/adolescence differed in clinical characteristics from those with onset during adulthood. To accomplish this, we divided the patients in two groups based on the ILAE guidelines (Wirrell et al., 2022); a childhood-onset TLE group (C-TLE) composed of patients who developed epilepsy before 18 years old, and an adult-onset group (A-TLE) characterized by those who developed seizures after age 18. C-TLE were characterized by a younger age and a longer disease duration compared to A-TLE. Moreover, C-TLE patients showed a higher frequency of HS compared to the A-TLE group. Conversely, the A-TLE were characterized by an older age and a shorter disease duration. There were no group differences in sex, education, ICV, and number of ASMs (see Table 3).

Due to group differences in age, sex, HS status, and education, we performed a secondary analysis within each group, controlling for these variables. This secondary analysis supported our original observations. In C-TLE, ipsilateral hippocampal volume loss was associated with increased ipsilateral SWM MD across the whole brain ($r = -0.426$, $p = 0.013$, Fig. 3**A**), in the temporal lobe (MTL: $r = -0.415$, $p = 0.016$; LTL: $r = -0.378$, $p = 0.030$), and in extra-temporal regions ($r = -0.354$, $p = .043$). As expected, there was no association between cortical thinning and SWM MD in the C-TLE group (Supplementary Table 5). On the other hand, in patients with A-TLE, cortical thinning was associated with greater SWM MD in the ipsilateral MTL ($r = -0.356$, $p = 0.024$), but there were no correlations in extra-temporal lobe regions, or between SWM MD and hippocampal atrophy ($r = -0.135$, $p = 0.406$, Fig. 3**B**, and Supplementary Table 5). Finally, these findings seemed to be related to TLE pathology as these associations were not found in controls (Fig. 3, and Supplementary Table 5).

Given the link between earlier seizure onset and a higher rate of HS (Davies et al., 1996), in a post-hoc analysis we explored the correlation between the age of the seizure onset and the volume of both hippocampi. As expected, lower volume in the ipsilateral hippocampus was correlated with younger age of onset ($r = 0.338$, $p = 0.002$), while volume of the contralateral hippocampus was not associated with age of onset ($r = 0.106$, $p = 0.345$). Therefore, we next examined whether hippocampal volume influences the observed relationship between age of seizure onset and SWM using a mediation analysis (Tingley et al., 2014). This analysis revealed non-significant overall (estimate $c = -0.0004$, $p = 0.884$) and direct (estimate $c' = -0.0004$, $p = 0.966$) effects, coupled with a significant indirect effect (estimate $a*b = -0.0078$, $p = 0.024$), such that the association between the age of seizure onset and SWM disruption was mediated by ipsilateral hippocampal volume (**Supplementary Figure 7**).

4. Discussion

The present study extends the literature by providing a comprehensive analysis of neocortical and subcortical GM and WM degeneration profiles in TLE and demonstrating how these patterns relate to one

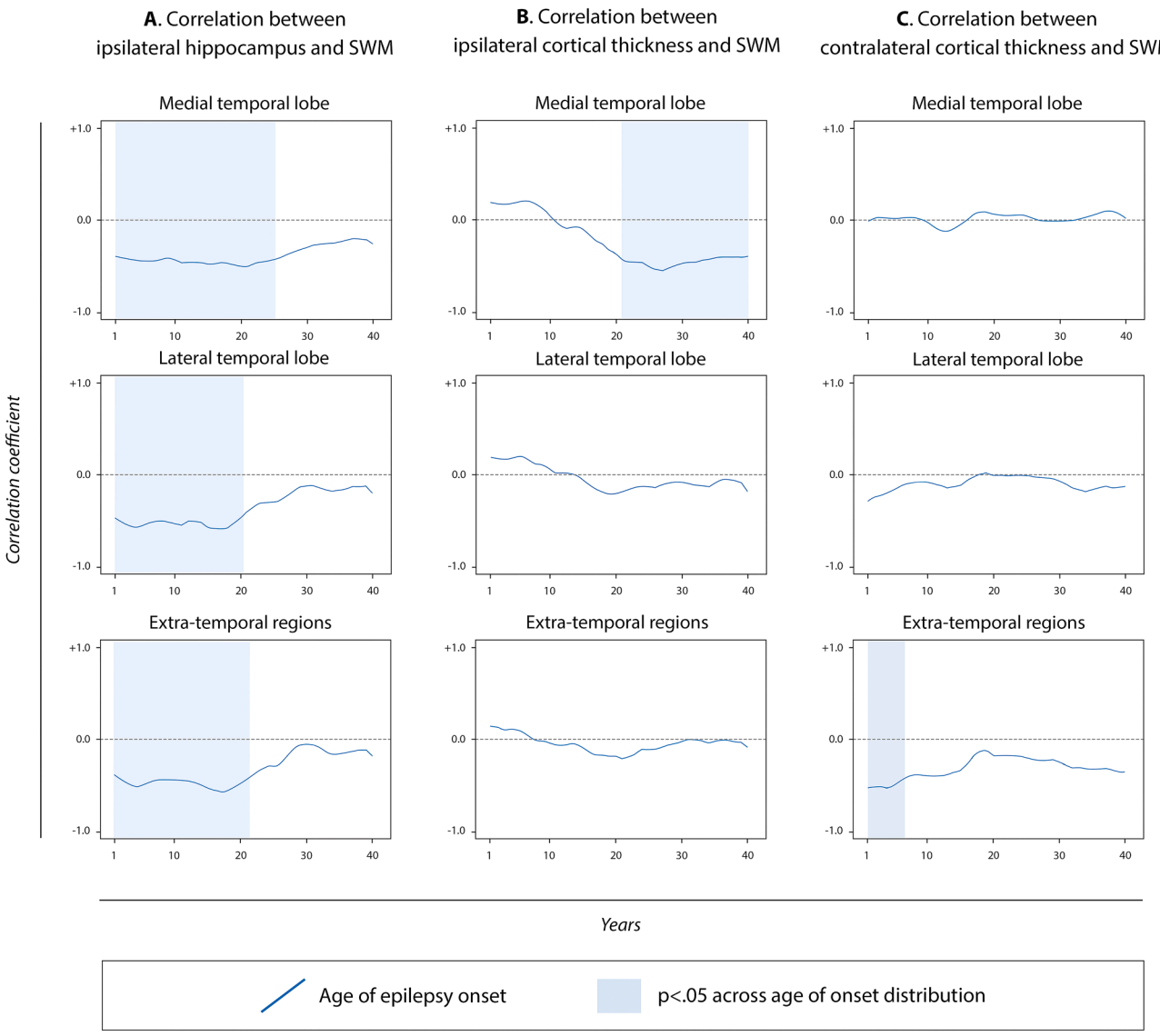

Fig. 2. *Sliding window correlations between brain measures in the TLE population as a function of the age of epilepsy onset.* Panel A) shows the association between SWM-MD and hippocampal volume in the ipsilateral hemisphere for the three main groups of regions. Panel B) shows the association between ipsilateral cortical thickness and SWM-MD for the three main groups of regions. Panel C) shows the same association between contralateral cortical thickness and SWM-MD for the same groups of regions. The blue lines display the correlation coefficients' fluctuation value across age of epilepsy onset, and the blue shading indicates when the relation is significant ($p < 0.05$). To ensure stability of the results, a bootstrapping analysis was applied to a random rank order of values to verify that the correlation values obtained were not due to chance. Thus, the p-values in the figure are uncorrected at each instance, reflecting the approach already described by Allen et al. (2014) and Shakil et al. (2018). A plot with the mean (±standard deviation) of the age of onset for each window is reported in **Supplementary Figure 5**. (For interpretation of the references to colour in this figure legend, the reader is referred to the web version of this article.)

another, to hippocampal volume, and to the seizure focus. At the whole group level, GM and WM patterns in TLE were spatially distinct. Cortical atrophy was observed to be widespread and bilateral, and most prominent in centro-parietal regions. Conversely, WM microstructural damage was mostly ipsilateral and temporo-limbic, following a similar pattern for both SWM and deep WM tracts. However, unique relationships emerged between GM and SWM pathology when groups were stratified by age of seizure onset, suggesting that different GM and WM structures are differentially impacted by TLE as a function of when seizures begin in life as well as the presence of hippocampal volume loss.

4.1. *The diffuse and widespread structural pathologies of TLE*

TLE is a focal epilepsy syndrome that nonetheless is associated with widespread and diffuse structural and microstructural damage (Hatton et al., 2020; Larivière et al., 2020; Park et al., 2022; Whelan et al., 2018) and abnormal connectivity patterns across most of the brain (Bernhardt et al., 2019; Liu et al., 2014; Tavakol et al., 2019). Much of the previous literature has focused on cortical thickness, hippocampal volumes, and deep WM tracts (Hatton et al., 2020; Larivière et al., 2020; Park et al., 2022; Whelan et al., 2018). Our findings complement previous reports (Chang et al., 2019; Liu et al., 2016) and highlight that, despite their proximity, cortical atrophy and SWM disruption appear to follow different spatial patterns of injury in TLE. Here, cortical thinning was widespread and bilateral, involving mostly of the posterior neocortex including the bilateral parietal and occipital lobes, especially in the bilateral precuneus, somatosensory and motor cortices. Furthermore, the ipsilateral MTL did not show prominent cortical thinning, which is also in line with previous reports (Larivière et al., 2020). This widespread multi-lobar cortical atrophy was instead characterized by a non-limbic and non-lateralized predominance (Larivière et al., 2020; McDonald et al., 2008; Whelan et al., 2018) suggesting that it arises from

Table 3
Clinical and demographic variables in C-TLE and A-TLE.

	C-TLE (N = 37)	A-TLE (N = 45)	Stat.	Sig.
Age	32.46(±13.617)	38.64(±11.798)	−2.203 [t]	0.030*
Sex (f/m)	24/13	20/25	3.405[X]	0.065
Education (y)	12.97(±1.724)	13.58(±2.179)	−1.371 [t]	0.174
ICV (mm^3)	979131.730 (±113650.017)	1000420.270 (±115629.576)	−0.836 [t]	0.406
TBV (mm^3)	1114386.657 (±127360.941)	1140873.702 (±129184.149)	−0.930 [t]	0.355
HS (yes/no)	27/10	20/25	6.755[X]	0.009**
Age of epilepsy onset (y)	8.30(±6.235)	30.93(±10.391)	−11.633 [t]	<0.001***
Epilepsy duration (y)	24.16(±15.645)	7.71(±6.808)	6.365 [t]	<0.001***
ASMs (mono/poly)	2.30(±0.909)	2.31(±0.925)	−0.068 [t]	0.946

Data are presented in means (±standard deviations). y: years, ICV: intracranial volume, TBV: total brain volume, HS: hippocampal sclerosis, ASM: anti-seizure medication. [t]: independent sample *t*-test, [X]: Chi-squared test, *: p <.05, **: p <.01, ***: p <.001.

processes independent of the seizure focus. This broad pattern of atrophy is supported by literature demonstrating similar patterns of cortical thinning across very different epilepsy syndromes (e.g., focal versus generalized), indicating that this may reflect a more general epilepsy-related phenomenon (Whelan et al., 2018). One recent study proposed that this spatial distribution of cortical atrophy could occur in those brain regions structurally connected with the hippocampus (i.e., pre and post central gyri, precuneus, lateral and medial temporal lobe) (Galovic et al., 2019). Nevertheless, this would not explain the full pattern observed in our study and requires replication in future studies.

In contrast to the cortical GM, the SWM showed a temporo-limbic pattern of degeneration that was mostly restricted to the ipsilateral hemisphere. Although FA was reduced in the inferomedial MTL only, MD anomalies extended to the ipsilateral orbitofrontal cortex, insula, and cingulate WM. This pattern of highly lateralized WM pathology was mirrored in the deep WM temporo-limbic tracts of the UNC, PHC, and FX where FA reductions were greater and MD increases were only observed in the ipsilateral fibers. These findings are supported by prior reports demonstrating an association between the seizure focus and proximal WM injury (Concha et al., 2012; Hatton et al., 2020; Urquia-Osorio et al., 2022). Our findings extend the literature by demonstrating that this pattern exists for both the SWM and deep WM association tracts.

4.2. Structural pathology and the developmental trajectory

Our results demonstrate spatially distinct patterns of neocortical and WM alterations in TLE patients in most brain regions, suggesting that different biological processes are likely driving these two types of injury. Data from animal models provide support for this, demonstrating that GM and WM are impacted along different timelines (Luna-Munguia et al., 2021; Roch et al., 2002b, 2002a), with cortical GM affected more acutely and WM affected over a longer time period following seizure onset. In addition, WM damage in chronic TLE models supports the idea of co-occurring damage in WM and hippocampal volume (Luna-Munguia et al., 2021). Previous research reported that SWM anomalies were mediated by hippocampal atrophy in TLE (Liu et al., 2016). Our results support and extend this finding, suggesting that hippocampal volume may mediate the relationship between age of seizure onset and SWM disruption. However, we suggest that a more complex relationship exists between cortical thinning, SWM loss, and hippocampal injury, which may be driven by the period of life during which seizures began. Indeed, SWM injury and hippocampal volume loss were highly related, but only for individuals with an early age of seizure onset. This relationship was maintained even after controlling for group imbalance in HS, suggesting that the WM damage was not merely a by-product of HS. Although WM and subcortical GM maturation reach their peak at different ages, changes in both are maximal between mid-gestation to adolescence (Bethlehem et al., 2022). Thus, the onset of seizures during this period could interfere with brain maturation, leading to concurrent hippocampal injury and disruption of WM development (Liu et al., 2016).

On the other hand, developing TLE in adulthood was associated with co-occurring cortical thinning and SWM injury, but only in the ipsilateral MTL. While cortical thinning begins in childhood and shows a relatively linear decrease across the lifespan in healthy individuals, SWM microstructure follows a similar pattern to the deep WM

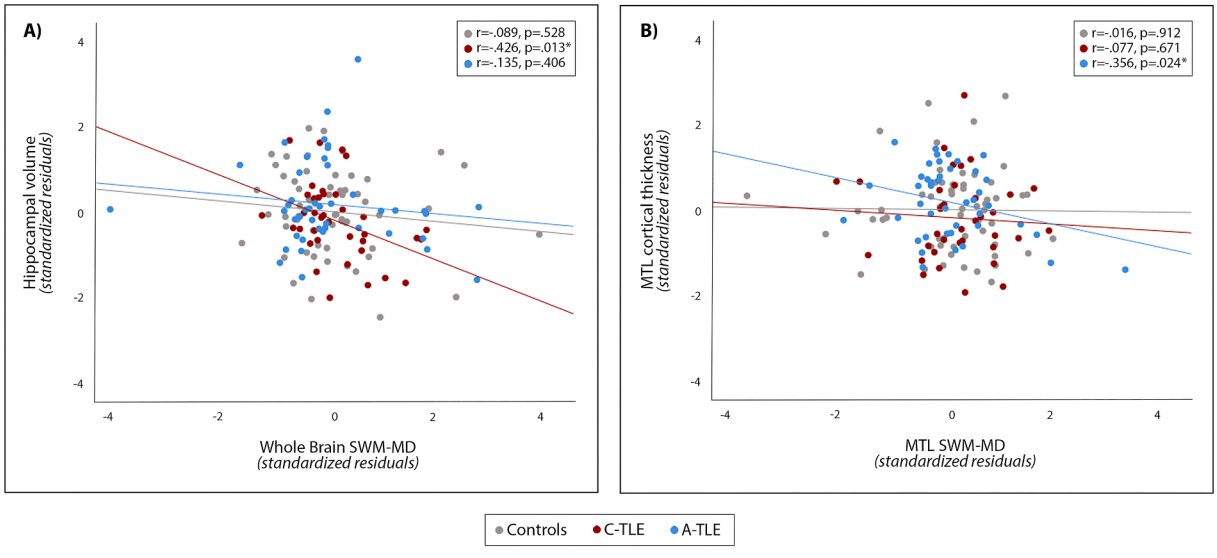

Fig. 3. *Partial correlations in controls, C-TLE (childhood-onset TLE) and A-TLE (adult-onset TLE) population.* Plot A) shows the correlation between hippocampal volume and whole brain SWM-MD. Plot B) shows the correlation between MTL cortical thickness and MTL SWM-MD. The scatterplots represent partial correlations between the brain measures corrected for age, sex, education, and HS status. Thus, the data are presented as standardized residuals. Gray dots and line are used to represent controls, red dots and line represent C-TLE, and blue dots and line represent A-TLE. SWM: superficial white matter, MD: mean diffusivity, MTL: medial temporal lobe, HS: hippocampal sclerosis, *: p <0.05. (For interpretation of the references to colour in this figure legend, the reader is referred to the web version of this article.)

association tracts with an increase in FA and decrease in MD that accelerates during adolescence, reaching a peak between 20 and 35 years of age (Bethlehem et al., 2022; Lebel et al., 2012; Schilling et al., 2022). In adulthood, SWM FA/MD levels off and then declines during late-adulthood (Schilling et al., 2022). Our results suggest that when TLE begins in adulthood, after the period of SWM peak development, it may lead to co-occurring and age-accelerated cortical and WM injury proximal to the epileptogenic zone. Interestingly, this is observed in TLE patients with a relatively short disease duration (**Supplementary Figure 5**), suggesting that these pathological changes may occur quite rapidly in drug-resistant adults and could underlie the progressive cognitive decline observed in many of these patients (Costa et al., 2019; Fernandes et al., 2022). Finally, all the results from the non-linear correlations highlighted effects only with respect to SWM MD, with no significant results found for FA. MD abnormalities refer to an overall tissue barrier impairment and degree of water diffusion within a voxel, with no orientation (Basser et al., 2000; Beaulieu, 2002). Thus, because of the convergence of deep and peripheral fibers with the SWM with less anisotropy than long WM bundles, MD may be a more sensitive marker of SWM microstructural disruption (Urquia-Osorio et al., 2022).

4.3. Limitations and future directions

Despite our novel findings, several limitations of our study should be addressed. First, we lack a cohort of older adults with TLE, preventing us from evaluating the impact of epilepsy on brain pathology across the adult lifespan. In particular, late onset epilepsy is defined as seizures that begin after the age of 55, often having a temporal lobe predominance, greater levels of MTL atrophy than observed in our current study, and often no clear etiology (Kaestner et al., 2021). Future studies should explore whether the pattern of structural pathology and its relationship across tissue types is affected by this very late age of seizure onset, and how these relationships may be related to cognitive decline and risk for dementia. Although our sample size is larger than many prior studies (Chang et al., 2019; Liu et al., 2016), a larger multi-center cohort would allow us to stratify patients by additional clinical and brain-related characteristics. First, this would enable us to better disentangle the roles of the age of seizure onset from the years of epilepsy duration. Age of seizure onset and duration of epilepsy were co-linear, and our analyses were cross-sectional, therefore limiting our ability to tease apart the unique effects of these two variables or understand the causality of the relationships. Moreover, a longitudinal study with a large cohort of patients who are heterogeneous in clinical characteristics would allow for a more enriched understanding of the mechanisms underlying TLE-related pathology. It is well known that FA, MD, cortical thickness, and volume have different maturation peaks during the lifespan (Bethlehem et al., 2022). In our secondary analysis, we clustered our sample into those with a pediatric vs adult age of seizure onset (i.e., before or after 18 years old), according to ILAE guidelines (Wirrell et al., 2022). A larger multi-center cohort would allow us to stratify our sample according to a range of brain maturation peaks and test our GM and WM relationships across various peaks. Finally, although we purport to replicate prior findings in our initial analysis of discordant GM and SWM patterns, it is of note that we used different methods for both extracting and summarizing our variables. However, we consider this a strength and believe that it provides evidence that these findings are robust to the methods employed.

5. Conclusion

Our data provide compelling evidence of a complex relationship between cortico-subcortical GM loss and WM injury in TLE; our findings suggest spatially unique patterns of cortical, hippocampal, and WM disruption. The age at which the seizures begin appears to influence the way in which these features are related to one another. Whereas the co-occurrence of hippocampal injury and WM damage in the ipsilateral hemisphere may be linked to neurodevelopmental factors, the onset of seizures in adulthood could set off a cascade of neurodegenerative changes, dominated by cortical atrophy and subcortical WM injury close to the epileptogenic zone.

6. Author's statement

We confirm that we have read the Journal's position on issues involved in ethical publication and affirm that this report is consistent with those guidelines. Data from our work will be made available upon request. Funding for this work was supported by NINDS (see Acknowledgements & Funding). None of the authors have any conflict of interest to disclose. This research was approved by the Institutional Review Boards at the University of California (UC) San Diego and UC San Francisco under a joint IRB plan. All participants provided informed consent according to the Declaration of Helsinki.

CRediT authorship contribution statement

Alice Ballerini: Conceptualization, Formal analysis, Methodology, Visualization, Writing – original draft. **Donatello Arienzo:** Methodology, Formal analysis, Writing – review & editing. **Alena Stasenko:** Writing – review & editing, Visualization. **Adam Schadler:** Data curation, Writing – review & editing. **Anna Elisabetta Vaudano:** Writing – review & editing. **Stefano Meletti:** Writing – review & editing. **Erik Kaestner:** Conceptualization, Project administration, Writing – original draft. **Carrie R. McDonald:** Conceptualization, Project administration, Writing – original draft.

Declaration of Competing Interest

The authors declare that they have no known competing financial interests or personal relationships that could have appeared to influence the work reported in this paper.

Acknowledgments & Funding

Erik Kaestner was funded by NINDS (K01NS12483). Alena Stasenko was funded by NINDS (F32 NS119285-02) and by an APA Society for Clinical Neuropsychology (Div. 40) Early Career Pilot Study Award. Carrie McDonald was founded by NIH/NINDS (R01 NS122827, R01 NS120976, and R01 NS065838). Stefano Meletti is supported by a grant "Dipartimenti di Eccellenza 2018-2022" (MIUR, Italy) to the Department of Biomedical, Metabolic and Neural Sciences and by a grant "Ricerca Finalizzata" (NET-2013-02355313) by Ministry of Health to the Azienda Ospedaliera-Universitaria di Modena "Centro Hub Chirurgia Epilessia" (DGR 1172/18).

Ethical publication statement

Anna Elisabetta Vaudano received personal compensation as scientific advisory board member for Angelini Pharma.

Appendix A. Supplementary data

Supplementary data to this article can be found online at https://doi.org/10.1016/j.nicl.2023.103473.

References

Allen, E.A., Damaraju, E., Plis, S.M., Erhardt, E.B., Eichele, T., Calhoun, V.D., 2014. Tracking Whole-Brain Connectivity Dynamics in the Resting State. Cerebral Cortex (New York, NY) 24 (3), 663–676. https://doi.org/10.1093/cercor/bhs352.

Andersson, J.L.R., Skare, S., Ashburner, J., 2003. How to correct susceptibility distortions in spin-echo echo-planar images: Application to diffusion tensor imaging. Neuroimage 20 (2), 870–888. https://doi.org/10.1016/S1053-8119(03)00336-7.

Basser, P.J., Pajevic, S., Pierpaoli, C., Duda, J., Aldroubi, A., 2000. In vivo fiber tractography using DT-MRI data. Magn. Reson. Med. 44 (4), 625–632. https://doi.org/10.1002/1522-2594(200010)44:4<625::AID-MRM17>3.0.CO;2-O.

Beaton, A.E., Tukey, J.W., 1974. The Fitting of Power Series, Meaning Polynomials, Illustrated on Band-Spectroscopic Data. Technometrics 16 (2), 147–185. https://doi.org/10.1080/00401706.1974.10489171.

Beaulieu, C., 2002. The basis of anisotropic water diffusion in the nervous system – a technical review. NMR Biomed. 15 (7–8), 435–455. https://doi.org/10.1002/nbm.782.

Beghi, E., 2020. The Epidemiology of Epilepsy. Neuroepidemiology 54 (2), 185–191. https://doi.org/10.1159/000503831.

Bencurova, P., Laakso, H., Salo, R.A., Paasonen, E., Manninen, E., Paasonen, J., Michaeli, S., Mangia, S., Bares, M., Brazdil, M., Kubova, H., Gröhn, O., 2022. Infantile status epilepticus disrupts myelin development. Neurobiol. Dis. 162, 105566 https://doi.org/10.1016/j.nbd.2021.105566.

Benjamini, Y., Hochberg, Y., 1995. Controlling the False Discovery Rate: A Practical and Powerful Approach to Multiple Testing. J. Roy. Stat. Soc.: Ser. B (Methodol.) 57 (1), 289–300. https://doi.org/10.1111/j.2517-6161.1995.tb02031.x.

Bernhardt, B.C., Fadaie, F., Liu, M., Caldairou, B., Gu, S., Jefferies, E., Smallwood, J., Bassett, D.S., Bernasconi, A., Bernasconi, N., 2019. Temporal lobe epilepsy: Hippocampal pathology modulates connectome topology and controllability. Neurology 92 (19), e2209–e2220. https://doi.org/10.1212/WNL.0000000000007447.

Bethlehem, R.A.I., Seidlitz, J., White, S.R., Vogel, J.W., Anderson, K.M., Adamson, C., Adler, S., Alexopoulos, G.S., Anagnostou, E., Areces-Gonzalez, A., Astle, D.E., Auyeung, B., Ayub, M., Bae, J., Ball, G., Baron-Cohen, S., Beare, R., Bedford, S.A., Benegal, V., Beyer, F., Blangero, J., Blesa Cábez, M., Boardman, J.P., Borzage, M., Bosch-Bayard, J.F., Bourke, N., Calhoun, V.D., Chakravarty, M.M., Chen, C., Chertavian, C., Chetelat, G., Chong, Y.S., Cole, J.H., Corvin, A., Costantino, M., Courchesne, E., Crivello, F., Cropley, V.L., Crosbie, J., Crossley, N., Delarue, M., Delorme, R., Desrivieres, S., Devenyi, G.A., Di Biase, M.A., Dolan, R., Donald, K.A., Donohoe, G., Dunlop, K., Edwards, A.D., Elison, J.T., Ellis, C.T., Elman, J.A., Eyler, L., Fair, D.A., Feczko, E., Fletcher, P.C., Fonagy, P., Franz, C.E., Galan-Garcia, L., Gholipour, A., Giedd, J., Gilmore, J.H., Glahn, D.C., Goodyer, I.M., Grant, P.E., Groenewold, N.A., Gunning, F.M., Gur, R.E., Gur, R.C., Hammill, C.F., Hansson, O., Hedden, T., Heinz, A., Henson, R.N., Heuer, K., Hoare, J., Holla, B., Holmes, A.J., Holt, R., Huang, H., Im, K., Ipser, J., Jack, C.R., Jackowski, A.P., Jia, T., Johnson, K.A., Jones, P.B., Jones, D.T., Kahn, R.S., Karlsson, H., Karlsson, L., Kawashima, R., Kelley, E.A., Kern, S., Kim, K.W., Kitzbichler, M.G., Kremen, W.S., Lalonde, F., Landeau, B., Lee, S., Lerch, J., Lewis, J.D., Li, J., Liao, W., Liston, C., Lombardo, M.V., Lv, J., Lynch, C., Mallard, T.T., Marcelis, M., Markello, R.D., Mathias, S.R., Mazoyer, B., McGuire, P., Meaney, M.J., Mechelli, A., Medic, N., Misic, B., Morgan, S.E., Mothersill, D., Nigg, J., Ong, M.Q.W., Ortinau, C., Ossenkoppele, R., Ouyang, M., Palaniyappan, L., Paly, L., Pan, P.M., Pantelis, C., Park, M.M., Paus, T., Pausova, Z., Paz-Linares, D., Pichet Binette, A., Pierce, K., Qian, X., Qiu, J., Qiu, A., Raznahan, A., Rittman, T., Rodrigue, A., Rollins, C.K., Romero-Garcia, R., Ronan, L., Rosenberg, M.D., Rowitch, D.H., Salum, G.A., Satterthwaite, T.D., Schaare, H.L., Schachar, R.J., Schultz, A.P., Schumann, G., Schöll, M., Sharp, D., Shinohara, R.T., Skoog, I., Smyser, C.D., Sperling, R.A., Stein, D.J., Stolicyn, A., Suckling, J., Sullivan, G., Taki, Y., Thyreau, B., Toro, R., Traut, N., Tsvetanov, K.A., Turk-Browne, N.B., Tuulari, J.J., Tzourio, C., Vachon-Presseau, É., Valdes-Sosa, M.J., Valdes-Sosa, P.A., Valk, S.L., van Amelsvoort, T., Vandekar, S.N., Vasung, L., Victoria, L.W., Villeneuve, S., Villringer, A., Vértes, P.E., Wagstyl, K., Wang, Y.S., Warfield, S.K., Warrier, V., Westman, E., Westwater, M.L., Whalley, H.C., Witte, A.V., Yang, N., Yeo, B., Yun, H., Zalesky, A., Zar, H.J., Zettergren, A., Zhou, J.H., Ziauddeen, H., Zugman, A., Zuo, X.N., Rowe, C., Frisoni, G.B., Binette, A.P., Bullmore, E.T., Alexander-Bloch, A.F., 2022. Brain charts for the human lifespan. Nature 604 (7906), 525–533.

Blümcke, I., Thom, M., Aronica, E., Armstrong, D.D., Bartolomei, F., Bernasconi, A., Bernasconi, N., Bien, C.G., Cendes, F., Coras, R., Cross, J.H., Jacques, T.S., Kahane, P., Mathern, G.W., Miyata, H., Moshé, S.L., Oz, B., Özkara, Ç., Perucca, E., Sisodiya, S., Wiebe, S., Spreafico, R., 2013. International consensus classification of hippocampal sclerosis in temporal lobe epilepsy: A Task Force report from the ILAE Commission on Diagnostic Methods. Epilepsia 54 (7), 1315–1329.

Bonilha, L., Edwards, J.C., Kinsman, S.L., Morgan, P.S., Fridriksson, J., Rorden, C., Rumboldt, Z., Roberts, D.R., Eckert, M.A., Halford, J.J., 2010. Extrahippocampal gray matter loss and hippocampal deafferentation in patients with temporal lobe epilepsy. Epilepsia 51 (4), 519–528. https://doi.org/10.1111/j.1528-1167.2009.02506.x.

Chang, Y.A., Marshall, A., Bahrami, N., Mathur, K., Javadi, S.S., Reyes, A., Hegde, M., Shih, J.J., Paul, B.M., Hagler, D.J., McDonald, C.R., 2019. Differential sensitivity of structural, diffusion, and resting-state functional MRI for detecting brain alterations and verbal memory impairment in temporal lobe epilepsy. Epilepsia 60 (5), 935–947. https://doi.org/10.1111/epi.14736.

Concha, L., Kim, H., Bernasconi, A., Bernhardt, B.C., Bernasconi, N., 2012. Spatial patterns of water diffusion along white matter tracts in temporal lobe epilepsy. Neurology 79 (5), 455–462. https://doi.org/10.1212/WNL.0b013e31826170b6.

Costa, B.S., Santos, M.C.V., Rosa, D.V., Schutze, M., Miranda, D.M., Romano-Silva, M.A., 2019. Automated evaluation of hippocampal subfields volumes in mesial temporal lobe epilepsy and its relationship to the surgical outcome. Epilepsy Res. 154, 152–156. https://doi.org/10.1016/j.eplepsyres.2019.05.011.

Davies, K.G., Hermann, B.P., Dohan, F.C., Foley, K.T., Bush, A.J., Wyler, A.R., 1996. Relationship of hippocampal sclerosis to duration and age of onset of epilepsy, and childhood febrile seizures in temporal lobectomy patients. Epilepsy Res. 24 (2), 119–126. https://doi.org/10.1016/0920-1211(96)00008-3.

Desikan, R.S., Ségonne, F., Fischl, B., Quinn, B.T., Dickerson, B.C., Blacker, D., Buckner, R.L., Dale, A.M., Maguire, R.P., Hyman, B.T., Albert, M.S., Killiany, R.J., 2006. An automated labeling system for subdividing the human cerebral cortex on MRI scans into gyral based regions of interest. Neuroimage 31 (3), 968–980. https://doi.org/10.1016/j.neuroimage.2006.01.021.

Doucet, G.E., Sharan, A., Pustina, D., Skidmore, C., Sperling, M.R., Tracy, J.I., 2015. Early and Late Age of Seizure Onset have a Differential Impact on Brain Resting-State Organization in Temporal Lobe Epilepsy. Brain Topogr. 28 (1), 113–126. https://doi.org/10.1007/s10548-014-0366-6.

Elman, J.A., Panizzon, M.S., Hagler, D.J., Fennema-Notestine, C., Eyler, L.T., Gillespie, N.A., Neale, M.C., Lyons, M.J., Franz, C.E., McEvoy, L.K., Dale, A.M., Kremen, W.S., 2017. Genetic and environmental influences on cortical mean diffusivity. Neuroimage 146, 90–99. https://doi.org/10.1016/j.neuroimage.2016.11.032.

Fernandes, M., Manfredi, N., Aluisantonio, L., Franchini, F., Chiaravalloti, A., Izzi, F., Di Santo, S., Schillaci, O., Mercuri, N.B., Placidi, F., Liguori, C., 2022. Cognitive functioning, cerebrospinal fluid Alzheimer's disease biomarkers and cerebral glucose metabolism in late-onset epilepsy of unknown aetiology: A prospective study. Eur. J. Neurosci. 56 (9), 5384–5396. https://doi.org/10.1111/ejn.15734.

Fischl, B., 2012. FreeSurfer. FreeSurfer. *NeuroImage* 62 (2), 774–781.

Fisher, R.S., Cross, J.H., French, J.A., Higurashi, N., Hirsch, E., Jansen, F.E., Lagae, L., Moshé, S.L., Peltola, J., Roulet Perez, E., Scheffer, I.E., Zuberi, S.M., 2017. Operational classification of seizure types by the International League Against Epilepsy: Position Paper of the ILAE Commission for Classification and Terminology. Epilepsia 58 (4), 522–530. https://doi.org/10.1111/epi.13670.

Galovic, M., van Dooren, V.Q.H., Postma, T.S., Vos, S.B., Caciagli, L., Borzì, G., Cueva Rosillo, J., Vuong, K.A., de Tisi, J., Nachev, P., Duncan, J.S., Koepp, M.J., 2019. Progressive Cortical Thinning in Patients With Focal Epilepsy. JAMA Neurol. 76 (10), 1230. https://doi.org/10.1001/jamaneurol.2019.1708.

Hagler, D.J., Ahmadi, M.E., Kuperman, J., Holland, D., McDonald, C.R., Halgren, E., Dale, A.M., 2009. Automated white-matter tractography using a probabilistic diffusion tensor atlas: Application to temporal lobe epilepsy. Hum. Brain Mapp. 30 (5), 1535–1547. https://doi.org/10.1002/hbm.20619.

Hagler, D.J., Hatton, SeanN., Cornejo, M.D., Makowski, C., Fair, D.A., Dick, A.S., Sutherland, M.T., Casey, B.J., Barch, D.M., Harms, M.P., Watts, R., Bjork, J.M., Garavan, H.P., Hilmer, L., Pung, C.J., Sicat, C.S., Kuperman, J., Bartsch, H., Xue, F., Heitzeg, M.M., Laird, A.R., Trinh, T.T., Gonzalez, R., Tapert, S.F., Riedel, M.C., Squeglia, L.M., Hyde, L.W., Rosenberg, M.D., Earl, E.A., Howlett, K.D., Baker, F.C., Soules, M., Diaz, J., de Leon, O.R., Thompson, W.K., Neale, M.C., Herting, M., Sowell, E.R., Alvarez, R.P., Hawes, S.W., Sanchez, M., Bodurka, J., Breslin, F.J., Morris, A.S., Paulus, M.P., Simmons, W.K., Polimeni, J.R., van der Kouwe, A., Nencka, A.S., Gray, K.M., Pierpaoli, C., Matochik, J.A., Noronha, A., Aklin, W.M., Conway, K., Glantz, M., Hoffman, E., Little, R., Lopez, M., Pariyadath, V., Weiss, S.R.B., Wolff-Hughes, D.L., DelCarmen-Wiggins, R., Feldstein Ewing, S.W., Miranda-Dominguez, O., Nagel, B.J., Perrone, A.J., Sturgeon, D.T., Goldstone, A., Pfefferbaum, A., Pohl, K.M., Prouty, D., Uban, K., Bookheimer, S.Y., Dapretto, M., Galvan, A., Bagot, K., Giedd, J., Infante, M.A., Jacobus, J., Patrick, K., Shilling, P.D., Desikan, R., Li, Y.i., Sugrue, L., Banich, M.T., Friedman, N., Hewitt, J.K., Hopfer, C., Sakai, J., Tanabe, J., Cottler, L.B., Nixon, S.J., Chang, L., Cloak, C., Ernst, T., Reeves, G., Kennedy, D.N., Heeringa, S., Peltier, S., Schulenberg, J., Sripada, C., Zucker, R.A., Iacono, W.G., Luciana, M., Calabro, F.J., Clark, D.B., Lewis, D.A., Luna, B., Schirda, C., Brima, T., Foxe, J.J., Freedman, E.G., Mruzek, D.W., Mason, M.J., Huber, R., McGlade, E., Prescot, A., Renshaw, P.F., Yurgelun-Todd, D.A., Allgaier, N.A., Dumas, J.A., Ivanova, M., Potter, A., Florsheim, P., Larson, C., Lisdahl, K., Charness, M.E., Fuemmeler, B., Hettema, J.M., Maes, H.H., Steinberg, J., Anokhin, A.P., Glaser, P., Heath, A.C., Madden, P.A., Baskin-Sommers, A., Constable, R.T., Grant, S.J., Dowling, G.J., Brown, S.A., Jernigan, T.L., Dale, A.M., 2019. Image processing and analysis methods for the Adolescent Brain Cognitive Development Study. Neuroimage 202, 116091.

Hatton, S. N., Huynh, K. H., Bonilha, L., Abela, E., Alhusaini, S., Altmann, A., Alvim, M. K. M., Balachandra, A. R., Bartolini, E., Bender, B., Bernasconi, N., Bernasconi, A., Bernhardt, B., Bargallo, N., Caldairou, B., Caligiuri, M. E., Carr, S. J. A., Cavalleri, G. L., Cendes, F., … McDonald, C. R. (2020). White matter abnormalities across different epilepsy syndromes in adults: An ENIGMA-Epilepsy study. *Brain*, *143*(8), 2454–2473. https://doi.org/10.1093/brain/awaa200.

Hermann, B., Seidenberg, M., Bell, B., Rutecki, P., Sheth, R., Ruggles, K., Wendt, G., O'Leary, D., Magnotta, V., 2002. The Neurodevelopmental Impact of Childhood-onset Temporal Lobe Epilepsy on Brain Structure and Function. Epilepsia 43 (9), 1062–1071. https://doi.org/10.1046/j.1528-1157.2002.49901.x.

Holland, D., Kuperman, J.M., Dale, A.M., 2010. Efficient correction of inhomogeneous static magnetic field-induced distortion in Echo Planar Imaging. Neuroimage 50 (1), 175–183. https://doi.org/10.1016/j.neuroimage.2009.11.044.

Horsley, J.J., Schroeder, G.M., Thomas, R.H., de Tisi, J., Vos, S.B., Winston, G.P., Duncan, J.S., Wang, Y., Taylor, P.N., 2022. Volumetric and structural connectivity abnormalities co-localise in TLE. NeuroImage: Clinical 35, 103105. https://doi.org/10.1016/j.nicl.2022.103105.

Jovicich, J., Czanner, S., Greve, D., Haley, E., van der Kouwe, A., Gollub, R., Kennedy, D., Schmitt, F., Brown, G., Macfall, J., Fischl, B., Dale, A., 2006. Reliability in multi-site structural MRI studies: Effects of gradient non-linearity correction on phantom and human data. Neuroimage 30 (2), 436–443. https://doi.org/10.1016/j.neuroimage.2005.09.046.

Kaestner, E., Reyes, A., Chen, A., Rao, J., Macari, A. C., Choi, J. Y., Qiu, D., Hewitt, K., Wang, Z. I., Drane, D. L., Hermann, B., Busch, R. M., Punia, V., McDonald, C. R., & Alzheimer's Disease Neuroimaging Initiative. (2021). Atrophy and cognitive profiles in older adults with temporal lobe epilepsy are similar to mild cognitive impairment. *Brain: A Journal of Neurology*, *144*(1), 236–250. https://doi.org/10.1093/brain/awaa397.

Kaestner, E., Reyes, A., Macari, A.C., Chang, Y., Paul, B.M., Hermann, B.P., McDonald, C. R., 2019. Identifying the neural basis of a language-impaired phenotype of temporal lobe epilepsy. Epilepsia 60 (8), 1627–1638. https://doi.org/10.1111/epi.16283.

Larivière, S., Paquola, C., Park, By., et al., 2021. The ENIGMA Toolbox multiscale neural contextualization of multisite neuroimaging datasets. Nat. Methods 18, 698–700. https://doi.org/10.1038/s41592-021-01186-4.

Larivière, S., Rodríguez-Cruces, R., Royer, J., Caligiuri, M.E., Gambardella, A., Concha, L., Keller, S.S., Cendes, F., Yasuda, C., Bonilha, L., Gleichgerrcht, E., Focke, N.K., Domin, M., von Podewills, F., Langner, S., Rummel, C., Wiest, R., Martin, P., Kotikalapudi, R., O'Brien, T.J., Sinclair, B., Vivash, L., Desmond, P.M., Alhusaini, S., Doherty, C.P., Cavalleri, G.L., Delanty, N., Kälviäinen, R., Jackson, G. D., Kowalczyk, M., Mascalchi, M., Semmelroch, M., Thomas, R.H., Soltanian-Zadeh, H., Davoodi-Bojd, E., Zhang, J., Lenge, M., Guerrini, R., Bartolini, E., Hamandi, K., Foley, S., Weber, B., Depondt, C., Absil, J., Carr, S.J.A., Abela, E., Richardson, M.P., Devinsky, O., Severino, M., Striano, P., Tortora, D., Hatton, S.N., Vos, S.B., Duncan, J.S., Whelan, C.D., Thompson, P.M., Sisodiya, S.M., Bernasconi, A., Labate, A., McDonald, C.R., Bernasconi, N., Bernhardt, B.C., 2020. Network-based atrophy modeling in the common epilepsies: A worldwide ENIGMA study. *Science*. Advances 6 (47). https://doi.org/10.1126/sciadv.abc6457.

Larivière, S., Royer, J., Rodríguez-Cruces, R., Paquola, C., Caligiuri, M.E., Gambardella, A., Concha, L., Keller, S.S., Cendes, F., Yasuda, C.L., Bonilha, L., Gleichgerrcht, E., Focke, N.K., Domin, M., von Podewills, F., Langner, S., Rummel, C., Wiest, R., Martin, P., Kotikalapudi, R., O'Brien, T.J., Sinclair, B., Vivash, L., Desmond, P.M., Lui, E., Vaudano, A.E., Meletti, S., Tondelli, M., Alhusaini, S., Doherty, C.P., Cavalleri, G.L., Delanty, N., Kälviäinen, R., Jackson, G. D., Kowalczyk, M., Mascalchi, M., Semmelroch, M., Thomas, R.H., Soltanian-Zadeh, H., Davoodi-Bojd, E., Zhang, J., Winston, G.P., Griffin, A., Singh, A., Tiwari, V.K., Kreilkamp, B.A.K., Lenge, M., Guerrini, R., Hamandi, K., Foley, S., Rüber, T., Weber, B., Depondt, C., Absil, J., Carr, S.J.A., Abela, E., Richardson, M.P., Devinsky, O., Severino, M., Striano, P., Tortora, D., Kaestner, E., Hatton, S.N., Vos, S. B., Caciagli, L., Duncan, J.S., Whelan, C.D., Thompson, P.M., Sisodiya, S.M., Bernasconi, A., Labate, A., McDonald, C.R., Bernasconi, N., Bernhardt, B.C., 2022. Structural network alterations in focal and generalized epilepsy assessed in a worldwide ENIGMA study follow axes of epilepsy risk gene expression. Nat. Commun. 13 (1) https://doi.org/10.1038/s41467-022-31730-5.

Lebel, C., Gee, M., Camicioli, R., Wieler, M., Martin, W., Beaulieu, C., 2012. Diffusion tensor imaging of white matter tract evolution over the lifespan. Neuroimage 60 (1), 340–352. https://doi.org/10.1016/j.neuroimage.2011.11.094.

Liu, M., Chen, Z., Beaulieu, C., Gross, D.W., 2014. Disrupted anatomic white matter network in left mesial temporal lobe epilepsy. Epilepsia 55 (5), 674–682. https://doi.org/10.1111/epi.12581.

Liu, M., Bernhardt, B.C., Hong, S.-J., Caldairou, B., Bernasconi, A., Bernasconi, N., 2016. The superficial white matter in temporal lobe epilepsy: A key link between structural and functional network disruptions. Brain 139 (9), 2431–2440. https://doi.org/10.1093/brain/aww167.

Luna-Munguia, H., Marquez-Bravo, L., Concha, L., 2021. Longitudinal changes in gray and white matter microstructure during epileptogenesis in pilocarpine-induced epileptic rats. Seizure 90, 130–140. https://doi.org/10.1016/j.seizure.2021.02.011.

McDonald, C.R., Hagler, D.J., Ahmadi, M.E., Tecoma, E., Iragui, V., Gharapetian, L., Dale, A.M., Halgren, E., 2008. Regional neocortical thinning in mesial temporal lobe epilepsy. Epilepsia 49 (5), 794–803. https://doi.org/10.1111/j.1528-1167.2008.01539.x.

Mueller, S., Laxer, K., Barakos, J., Ian, C., Garcia, P., Weiner, M., 2009. Widespread Neocortical Abnormalities in Temporal Lobe Epilepsy With And Without Mesial Sclerosis. Neuroimage 46 (2), 353–359. https://doi.org/10.1016/j.neuroimage.2009.02.020.

Nagy, S.A., Horváth, R., Perlaki, G., Orsi, G., Barsi, P., John, F., Horváth, A., Kovács, N., Bogner, P., Ábrahám, H., Bóné, B., Gyimesi, C., Dóczi, T., Janszky, J., 2016. Age at onset and seizure frequency affect white matter diffusion coefficient in patients with mesial temporal lobe epilepsy. Epilepsy Behav. 61, 14–20. https://doi.org/10.1016/j.yebeh.2016.04.019.

Park, B., Larivière, S., Rodríguez-Cruces, R., Royer, J., Tavakol, S., Wang, Y., Caciagli, L., Caligiuri, M. E., Gambardella, A., Concha, L., Keller, S. S., Cendes, F., Alvim, M. K. M., Yasuda, C., Bonilha, L., Gleichgerrcht, E., Focke, N. K., Kreilkamp, B. A. K., Domin, M., … Bernhardt, B. C. (2022). Topographic divergence of atypical cortical asymmetry and atrophy patterns in temporal lobe epilepsy. *Brain*, *145*(4), 1285–1298. https://doi.org/10.1093/brain/awab417.

Reyes, A., Kaestner, E., Ferguson, L., Jones, J.E., Seidenberg, M., Barr, W.B., Busch, R.M., Hermann, B.P., McDonald, C.R., 2020. Cognitive phenotypes in temporal lobe epilepsy utilizing data- and clinically driven approaches: Moving toward a new taxonomy. Epilepsia 61 (6), 1211–1220. https://doi.org/10.1111/epi.16528.

Roch, C., Leroy, C., Nehlig, A., Namer, I.J., 2002a. Magnetic Resonance Imaging in the Study of the Lithium-Pilocarpine Model of Temporal Lobe Epilepsy in Adult Rats. Epilepsia 43 (4), 325–335. https://doi.org/10.1046/j.1528-1157.2002.11301.x.

Roch, C., Leroy, C., Nehlig, A., Namer, I.J., 2002b. Predictive Value of Cortical Injury for the Development of Temporal Lobe Epilepsy in 21-day-old Rats: An MRI Approach Using the Lithium-pilocarpine Model. Epilepsia 43 (10), 1129–1136. https://doi.org/10.1046/j.1528-1157.2002.17802.x.

Scheffer, I.E., Berkovic, S., Capovilla, G., Connolly, M.B., French, J., Guilhoto, L., Hirsch, E., Jain, S., Mathern, G.W., Moshé, S.L., Nordli, D.R., Perucca, E., Tomson, T., Wiebe, S., Zhang, Y.-H., Zuberi, S.M., 2017. ILAE classification of the epilepsies: Position paper of the ILAE Commission for Classification and Terminology. Epilepsia 58 (4), 512–521. https://doi.org/10.1111/epi.13709.

Schilling, K. G., Archer, D., Rheault, F., Lyu, I., Huo, Y., Cai, L. Y., Bunge, S. A., Weiner, K. S., Gore, J. C., Anderson, A. W., & Landman, B. A. (2022). Superficial white matter across the lifespan: Volume, thickness, change, and relationship with cortical features. *BioRxiv*, 2022.07.20.500818. https://doi.org/10.1101/2022.07.20.500818.

Schulz, D., Huston, J.P., 2002. The sliding window correlation procedure for detecting hidden correlations: Existence of behavioral subgroups illustrated with aged rats. J. Neurosci. Methods 121 (2), 129–137. https://doi.org/10.1016/S0165-0270(02)00224-8.

Shakil, S., Billings, J.C., Keilholz, S.D., Lee, C.-H., 2018. Parametric Dependencies of Sliding Window Correlation. I.E.E.E. Trans. Biomed. Eng. 65 (2), 254–263. https://doi.org/10.1109/TBME.2017.2762763.

Smith, S.M., Jenkinson, M., Woolrich, M.W., Beckmann, C.F., Behrens, T.E.J., Johansen-Berg, H., Bannister, P.R., De Luca, M., Drobnjak, I., Flitney, D.E., Niazy, R.K., Saunders, J., Vickers, J., Zhang, Y., De Stefano, N., Brady, J.M., Matthews, P.M., 2004. Advances in functional and structural MR image analysis and implementation as FSL. Neuroimage 23 (Suppl 1), S208–S219. https://doi.org/10.1016/j.neuroimage.2004.07.051.

Stasenko, A., Lin, C., Bonilha, L., Bernhardt, B.C., McDonald, C.R., 2022. Neurobehavioral and Clinical Comorbidities in Epilepsy: The Role of White Matter Network Disruption. Neuroscientist 10738584221076132. https://doi.org/10.1177/10738584221076133.

Tavakol, S., Royer, J., Lowe, A.J., Bonilha, L., Tracy, J.I., Jackson, G.D., Duncan, J.S., Bernasconi, A., Bernasconi, N., Bernhardt, B.C., 2019. Neuroimaging and connectomics of drug-resistant epilepsy at multiple scales: From focal lesions to macroscale networks. Epilepsia 60 (4), 593–604. https://doi.org/10.1111/epi.14688.

Tingley, D., Yamamoto, T., Hirose, K., Keele, L., Imai, K., 2014. mediation: R Package for Causal Mediation Analysis. J. Stat. Softw. 59, 1–38. https://doi.org/10.18637/jss.v059.i05.

Urquia-Osorio, H., Pimentel-Silva, L.R., Rezende, T.J.R., Almendares-Bonilla, E., Yasuda, C.L., Concha, L., Cendes, F., 2022. Superficial and deep white matter diffusion abnormalities in focal epilepsies. Epilepsia 63 (9), 2312–2324.

Whelan, C.D., Altmann, A., Botía, J.A., Jahanshad, N., Hibar, D.P., Absil, J., Alhusaini, S., Alvim, M.K.M., Auvinen, P., Bartolini, E., Bergo, F.P.G., Bernardes, T., Blackmon, K., Braga, B., Caligiuri, M.E., Calvo, A., Carr, S.J., Chen, J., Chen, S., Cherubini, A., David, P., Domin, M., Foley, S., França, W., Haaker, G., Isaev, D., Keller, S.S., Kotikalapudi, R., Kowalczyk, M.A., Kuzniecky, R., Langner, S., Lenge, M., Leyden, K. M., Liu, M., Loi, R.Q., Martin, P., Mascalchi, M., Morita, M.E., Pariente, J.C., Rodríguez-Cruces, R., Rummel, C., Saavalainen, T., Semmelroch, M.K., Severino, M., Thomas, R.H., Tondelli, M., Tortora, D., Vaudano, A.E., Vivash, L., von Podewils, F., Wagner, J., Weber, B., Yao, Y.i., Yasuda, C.L., Zhang, G., Bargalló, N., Bender, B., Bernasconi, N., Bernasconi, A., Bernhardt, B.C., Blümcke, I., Carlson, C., Cavalleri, G. L., Cendes, F., Concha, L., Delanty, N., Depondt, C., Devinsky, O., Doherty, C.P., Focke, N.K., Gambardella, A., Guerrini, R., Hamandi, K., Jackson, G.D., Kälviäinen, R., Kochunov, P., Kwan, P., Labate, A., McDonald, C.R., Meletti, S., O'Brien, T.J., Ourselin, S., Richardson, M.P., Striano, P., Thesen, T., Wiest, R., Zhang, J., Vezzani, A., Ryten, M., Thompson, P.M., Sisodiya, S.M., 2018. Structural brain abnormalities in the common epilepsies assessed in a worldwide ENIGMA study. Brain 141 (2), 391–408.

Winston, G.P., Vos, S.B., Caldairou, B., Hong, S.-J., Czech, M., Wood, T.C., Wastling, S.J., Barker, G.J., Bernhardt, B.C., Bernasconi, N., Duncan, J.S., Bernasconi, A., 2020. Microstructural imaging in temporal lobe epilepsy: Diffusion imaging changes relate to reduced neurite density. NeuroImage: Clinical 26, 102231. https://doi.org/10.1016/j.nicl.2020.102231.

Wirrell, E.C., Nabbout, R., Scheffer, I.E., Alsaadi, T., Bogacz, A., French, J.A., Hirsch, E., Jain, S., Kaneko, S., Riney, K., Samia, P., Snead, O.C., Somerville, E., Specchio, N., Trinka, E., Zuberi, S.M., Balestrini, S., Wiebe, S., Cross, J.H., Perucca, E., Moshé, S.L., Tinuper, P., 2022. Methodology for classification and definition of epilepsy syndromes with list of syndromes: Report of the ILAE Task Force on Nosology and Definitions. Epilepsia 63 (6), 1333–1348.

Zhuang, J., Hrabe, J., Kangarlu, A., Xu, D., Bansal, R., Branch, C.A., Peterson, B.S., 2006. Correction of Eddy-Current Distortions in Diffusion Tensor Images Using the Known Directions and Strengths of Diffusion Gradients. Journal of Magnetic Resonance Imaging : JMRI 24 (5), 1188–1193. https://doi.org/10.1002/jmri.20727.